Clay hypoplasticity model with explicit asymptotic state boundary surface formulation and very small strain stiffness anisotropy

D. Mašín
Faculty of Science
Charles University in Prague, Czech Republic

ABSTRACT: Hypoplastic model for clays is presented which predicts anisotropy of very small strain stiffness. The existing hypoplastic model with explicit formulation of the asymptotic state boundary surface is combined with an anisotropic form of the stiffness tensor. Naturally, the resultant model predicts correctly the very small strain stiffness anisotropy. It is demonstrated that properly are also predicted trends in the anisotropy influence on undrained stress paths. The model is evaluated using hollow cylinder apparatus experimental data on London clay taken over from literature.

INTRODUCTION

Anisotropy of sedimentary clays is such a significant feature of their mechanical behaviour that it cannot be ignored in boundary value problem simulations. For example, Addenbrooke et al. (1997), Gunn (1993), Ng et al. (2004) and Franzius et al. (2005) demonstrated that incorporation of stiffness anisotropy improved predictions of tunnelling problems. In this paper, we present a hypoplastic model for clays incorporating very small strain stiffness anisotropy recently developed by Mašín (2013). The model is also capable of predicting small strain stiffness non-linearity, recent stress history effects and large-strain asymptotic behaviour (Gudehus and Mašín 2009, Mašín 2012a), which are features inherited from the reference model with isotropic stiffness.

Hypoplasticity is an approach to non-linear constitutive modelling of geomaterials. In its general form by Gudehus (1996) it may be written as

$$\mathring{\boldsymbol{\sigma}} = f_s \left(\boldsymbol{\mathcal{L}} : \dot{\boldsymbol{\epsilon}} + f_d \mathbf{N} \| \dot{\boldsymbol{\epsilon}} \| \right) \tag{1}$$

where $\mathring{\boldsymbol{\sigma}}$ and $\dot{\boldsymbol{\epsilon}}$ represent the objective (Zaremba-Jaumann) stress rate and the Euler stretching tensor respectively, $\mathcal{L}$ and $\mathbf{N}$ are fourth- and second-order constitutive tensors, and f_s and f_d are two scalar factors. In hypoplasticity, stiffness predicted by the model is controlled by the tensor $\mathcal{L}$, while strength (and asymptotic response in general, see Mašín 2012a), is governed by a combination of $\mathcal{L}$ and $\mathbf{N}$. Earlier hypoplastic models, such as models by von Wolffersdorff (1996) and Mašín (2005), did not allow to adjust the $\mathcal{L}$ formulation freely, as any modification of tensor $\mathcal{L}$ undesirably influenced the predicted asymptotic states. This hypoplasticity limitation was overcome by Mašín (2012c). He developed an approach enabling to specify the asymptotic state boundary surface independently of the tensor $\mathcal{L}$ and demonstrated it by proposing a simple hypoplastic equivalent of the Modified Cam-clay model. Based this approach, Mašín (2012b) developed an advanced hypoplastic model for clays. This model serves as an underlining model for the presented model incorporating stiffness anisotropy. For further details of hypoplastic modelling, the readers are referred to the above-cited publications.

MODEL FORMULATION

The model presented in this paper combines hypoplastic model from Mašín (2012b) with anisotropic form of the tensor $\mathcal{L}$ proposed by Mašín & Rott (2013). Mašín & Rott (2013) adopted general transversely elastic model formulation, which reads (Spencer 1982, Lubarda & Chen 2008)

$$\mathcal{L} = \frac{1}{2} a_1 \mathbf{1} \circ \mathbf{1} + a_2 \mathbf{1} \otimes \mathbf{1} + a_3 \left(\boldsymbol{p} \otimes \mathbf{1} + \mathbf{1} \otimes \boldsymbol{p} \right) + \\ + a_4 \boldsymbol{p} \circ \mathbf{1} + a_5 \boldsymbol{p} \otimes \boldsymbol{p} \tag{2}$$

where the tensor products represented by "$\otimes$" and "$\circ$" are defined as

$$\left(\boldsymbol{p} \otimes \mathbf{1} \right)_{ijkl} = p_{ij} 1_{kl} \tag{3}$$

$$\left(\boldsymbol{p} \circ \mathbf{1} \right)_{ijkl} = \frac{1}{2} \left(p_{ik} 1_{jl} + p_{il} 1_{jk} + p_{jl} 1_{ik} + p_{jk} 1_{il} \right) \tag{4}$$

where $p_{ij} = n_i n_j$, while n_i is a unit vector normal to the plane of symmetry (in sedimentary soils this vector typically represents the vertical direction). a_1 to a_5 in Eq. (2) represent five material constants. They are defined as

$$a_1 = \alpha_E \left(1 - \nu_{pp} - 2\frac{\alpha_E}{\alpha_\nu^2}\nu_{pp}^2\right) \tag{5}$$

$$a_2 = \alpha_E \nu_{pp} \left(1 + \frac{\alpha_E}{\alpha_\nu^2}\nu_{pp}\right) \tag{6}$$

$$a_3 = \alpha_E \nu_{pp} \left(\frac{1}{\alpha_\nu} + \frac{\nu_{pp}}{\alpha_\nu} - 1 - \frac{\alpha_E}{\alpha_\nu^2}\nu_{pp}\right) \tag{7}$$

$$a_4 = \alpha_E \left(1 - \nu_{pp} - 2\frac{\alpha_E}{\alpha_\nu^2}\nu_{pp}^2\right) \frac{1-\alpha_G}{\alpha_G} \tag{8}$$

$$a_5 = \alpha_E \left(1 - \frac{\alpha_E}{\alpha_\nu^2}\nu_{pp}^2\right) + 1 - \nu_{pp}^2 - \tag{9}$$

$$-2\frac{\alpha_E}{\alpha_\nu}\nu_{pp}\left(1+\nu_{pp}\right) - \frac{2\alpha_E}{\alpha_G}\left(1 - \nu_{pp} - 2\frac{\alpha_E}{\alpha_\nu^2}\nu_{pp}^2\right)$$

where the anisotropy coefficients α_G, α_E and α_ν read

$$\alpha_G = \frac{G_{pp}}{G_{tp}} \tag{10}$$

$$\alpha_E = \frac{E_p}{E_t} \tag{11}$$

$$\alpha_\nu = \frac{\nu_{pp}}{\nu_{tp}} \tag{12}$$

G_{ij} are shear moduli, E_i are Young moduli and ν_{ij} are Poisson ratios. Subscript "$_p$" denotes direction within the plane of isotropy (typically horisontal direction) and subscript "$_t$" denotes direction transverse to the plane of isotropy (typically vertical direction). As suggested by Mašín & Rott (2013), parameters α_E and α_ν may be estimated using empirical correlations

$$\alpha_E = \alpha_G^{(1/x_{GE})} \tag{13}$$

$$\alpha_\nu = \alpha_G^{(1/x_{G\nu})} \tag{14}$$

with $x_{GE} = 0.8$ and $x_{G\nu} = 1$.

When compared to the reference model, incorporation of anisotropic form of $\mathcal{L}$ requires re-evaluation of the factor f_s from (1). According to Mašín (2012c), this factor may be quantified by comparing the isotropic unloading formulation of the hypoplastic model with the isotropic unloading line of the predefined form

$$\frac{\dot{e}}{1+e} = -\kappa^* \frac{\dot{p}}{p} \tag{15}$$

The isotropic version of the model is obtained by algebraic manipulations with (1), for details see Mašín (2013).

$$\dot{p} = \left(\frac{p}{\lambda^*} - 2f_s\frac{A_m}{9}\right)\frac{\dot{e}}{1+e} \tag{16}$$

where

$$A_m = \nu_{pp}^2\left(\frac{4\alpha_E}{\alpha_\nu} - 2\alpha_E^2 + 2\frac{\alpha_E^2}{\alpha_\nu^2} - 1\right) + \\ + \nu_{pp}\left(\frac{4\alpha_E}{\alpha_\nu} + 2\alpha_E\right) + 2\alpha_E + 1 \tag{17}$$

Comparison of (16) with (15) then yields

$$f_s = -\frac{3\,\mathrm{tr}\,\boldsymbol{\sigma}}{2A_m}\left(\frac{1}{\lambda^*} + \frac{1}{\kappa^*}\right) \tag{18}$$

The proposed model reduces to the reference one for $\alpha_G = \alpha_E = \alpha_\nu = 1$.

To predict very small strain stiffness and recent stress history effects, the model must be combined with the intergranular strain concept by Niemunis & Herle (1997). The very small strain stiffness matrix $\mathcal{M}_0$ then reads

$$\mathcal{M}_0 = m_R f_s \boldsymbol{\mathcal{L}} \tag{19}$$

The shear G_{tp0} component of the tensor $\mathcal{M}_0$ is given by (from (2), (17) and (18))

$$G_{tp0} = m_R \frac{9p}{2A_m}\left(\frac{1}{\lambda^*} + \frac{1}{\kappa^*}\right)\frac{\alpha_E}{2\alpha_G} * \\ * \left(1 - \nu_{pp} - 2\frac{\alpha_E}{\alpha_\nu^2}\nu_{pp}^2\right) \tag{20}$$

In the present work, we consider the following dependency of G_{tp0} on mean stress p (Wroth and Houlsby 1985)

$$G_{tp0} = p_r A_g \left(\frac{p}{p_r}\right)^{n_g} \tag{21}$$

where A_g and n_g are parameters and p_r is a reference pressure of 1 kPa. Comparison of (20) and (21) yields the following expression for the variable[1] m_R.

$$m_R = p_r A_g \left(\frac{p}{p_r}\right)^{n_g} \frac{4A_m\alpha_G}{9p\alpha_E}\left(\frac{\lambda^*\kappa^*}{\lambda^*+\kappa^*}\right) * \\ * \frac{1}{1 - \nu_{pp} - 2\frac{\alpha_E}{\alpha_\nu^2}\nu_{pp}^2} \tag{22}$$

Complete model formulation is presented in the journal publication (Mašín 2013). Its finite element implementation is freely available on the web (Gudehus et al. 2008).

[1] Note that in the original intergranular strain concept formulation, m_R is considered as a parameter. Contrary, in the formulation proposed here, m_R is a variable calculated on the basis of G_{tp0} expression (21).

EVALUATION OF THE MODEL

The proposed model has been evaluated using extensive experimental data set on London clay from Imperial College project by Nishimura et al. (2007), Nishimura (2005), Gasparre et al. (2007) and Gasparre (2005). They tested undisturbed samples of London clay from the excavation at Heathrow, Terminal 5. In the evaluation, we used hollow cylinder tests on London clay from the depth of 10.5 m. Two sets of experiments have been simulated. In the first one, the soil was isotropically consolidated to the *in-situ* effective stress of $p' = 323$ kPa (series "IC" by Nishimura et al. 2007). In the second one, the initial conditions represented the estimated anisotropic *in-situ* stress state of $p' = 323$ kPa and $q = -166$ kPa (series "AC" by Nishimura et al. 2007). In both cases, the soil was sheared after consolidation under undrained conditions with controlled vertical strain. Total stress path was defined by constant total mean stress and constant values of variables $\alpha_{d\sigma}$ and b. These were defined as

$$\alpha_{d\sigma} = \frac{1}{2}\tan^{-1}\left(\frac{2\Delta\tau_{z\theta}}{\Delta\sigma_z - \Delta\sigma_\theta}\right) \tag{23}$$

$$b = \frac{\sigma_2 - \sigma_3}{\sigma_1 - \sigma_3} \tag{24}$$

where σ_1, σ_2 and σ_3 are the major, intermediate and minor principal stresses respectively and σ_z, σ_θ and $\tau_{z\theta}$ are rectilinear stress components in the specimen frame of reference (see Nishimura et al. 2007). Notation of stress state within the hollow cylinder specimen is clarified in Fig. 1. The value of b represents the contribution of the intermediate principal stress such that in the standard compression experiment in triaxial apparatus $b = 0$. Only simulations with $b = 0.5$ are presented here for brevity. $\alpha_{d\sigma}$ represents the principal stress inclination revealing soil anisotropy. In the standard triaxial test, $\alpha_{d\sigma} = 0°$ for the vertically trimmed specimen and $\alpha_{d\sigma} = 90°$ for the horizontally trimmed specimen.

The parameters φ_c, λ^* and κ^*, calibrated using data by Gasparre (2005), were taken over from Mašín (2009). The parameter N was adjusted so that the soil overconsolidation manifested by the undrained stress paths was predicted properly. The initial value of void ratio $e = 0.69$ was calculated from the specimen water content and specific gravity provided by Nishimura et al. (2007). The parameters A_g, n_g and α_G were calibrated using resonant column apparatus tests on London clay, as demonstrated in Figs. 2 and 3. Empirical expressions were adopted for α_E (13) and α_ν (14). ν_{pp} was estimated using stress-strain curves of shear tests at large strains, see Fig. 4. Intergranular strain parameters R, β_r and χ were calibrated using stiffness degradation curves from hollow cylinder tests. An example of such a curve is given in Fig. 5.

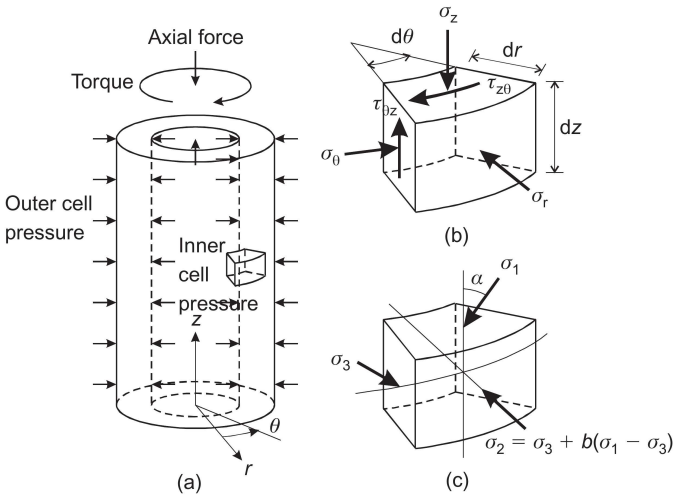

Figure 1: Stress state within the hollow cylinder specimen (figure from Nishimura et al., 2007).

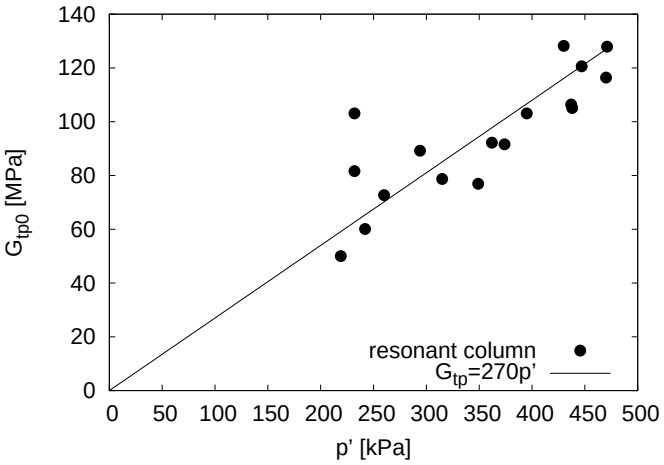

Figure 2: Calibration of the parameters A_g and n_g using resonant column apparatus experiments by Nishimura (2005).

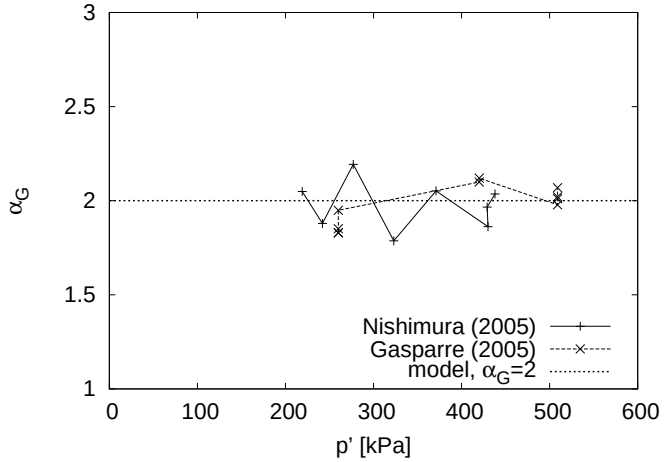

Figure 3: α_G calibration based on experiments by Nishimura (2005) and Gasparre (2005).

The material parameters adopted in all the simulations are in Tabs. 1 and 2. Predictions by the proposed model have been compared with predictions by the model by Mašín (2005).

Stress paths of various tests are in the p' vs. $(\sigma_z - \sigma_\theta)/2$ stress space plotted in Fig. 6. Stress-strain curves (q/p' vs. the principal strain difference $\epsilon_1 - \epsilon_3$) are presented in Figs. 7 and 8. The soil anisotropy

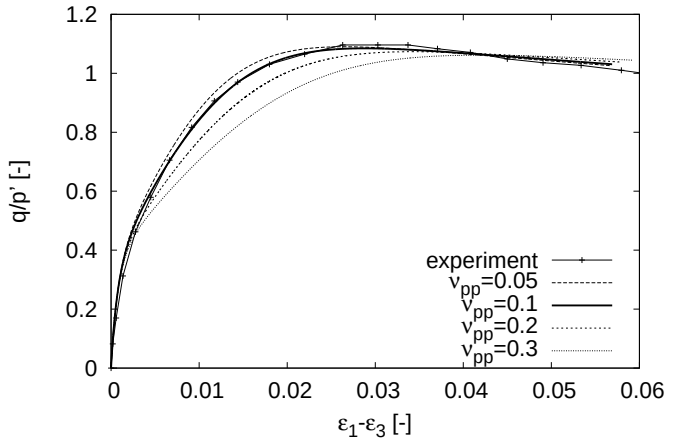

Figure 4: The influence of the parameter ν_{pp} on the ratio q/p' vs. the principal strain difference $\epsilon_1 - \epsilon_3$ curve in hollow cylinder test with $\alpha_{d\sigma} = 23°$ and $b = 0.5$. Experimental data by Nishimura (2005).

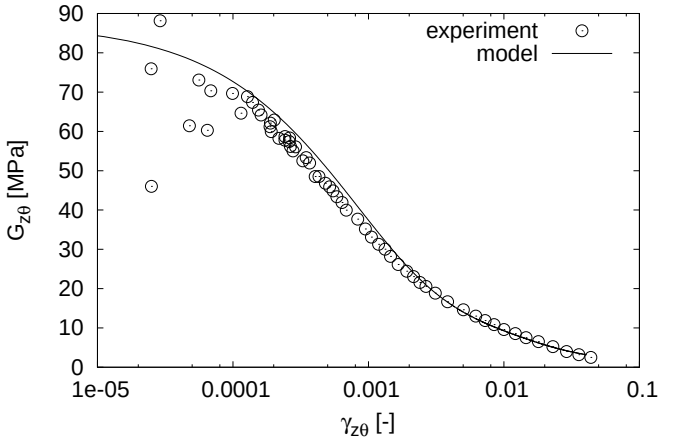

Figure 5: Secant shear stiffness degradation as measured by Nishimura (2005) in hollow cylinder test with $\alpha_{d\sigma} = 23°$ and $b = 0.5$ and predictions by the proposed model.

is revealed by the deviation of the stress path from vertical (constant p'). The proposed model predicts the stress path inclination properly for both isotropically and anisotropically consolidated specimens. The stress paths deviate from the experimental after the peak of q/p', but this may be explained by the specimen rupture and strain localisation into shear bands (see Nishimura et al. (2007) for indication of the pre-rupture stress path portions). Predictions by the model by Mašín (2005) are also shown in Figs. 6, 7 and 8

Table 1: *Parameters of the intergranular strain concept by Niemunis and Herle (1997) adopted in combination with different hypoplastic models.*

	A_g/m_R	n_g	m_{rat}/m_T
proposed model	$A_g = 270$	1	$m_{rat} = 0.5$
Mašín (2005) model	$m_R = 8$	n/a	$m_T = 4$
	R	β_r	χ
proposed model	5×10^{-5}	0.08	0.9
Mašín (2005) model	5×10^{-5}	0.08	0.9

Table 2: *Parameters of the hypoplastic models used in simulations.*

	φ_c	λ^*	κ^*
proposed model	$21.9°$	0.095	0.015
Mašín (2005) model	$21.9°$	0.095	0.015
	N	ν_{pp}/r	α
proposed model	1.19	$\nu_{pp} = 0.1$	2
Mašín (2005) model	1.19	$r = 0.3$	n/a

for comparison. This model predicts some degree of stress-induced anisotropy in the anisotropically consolidated specimens, but its degree cannot be controlled by a parameter and in the present case it is clearly underestimated. The response of the isotropically consolidated specimens is incorrectly predicted as initially isotropic by the Mašín (2005) model.

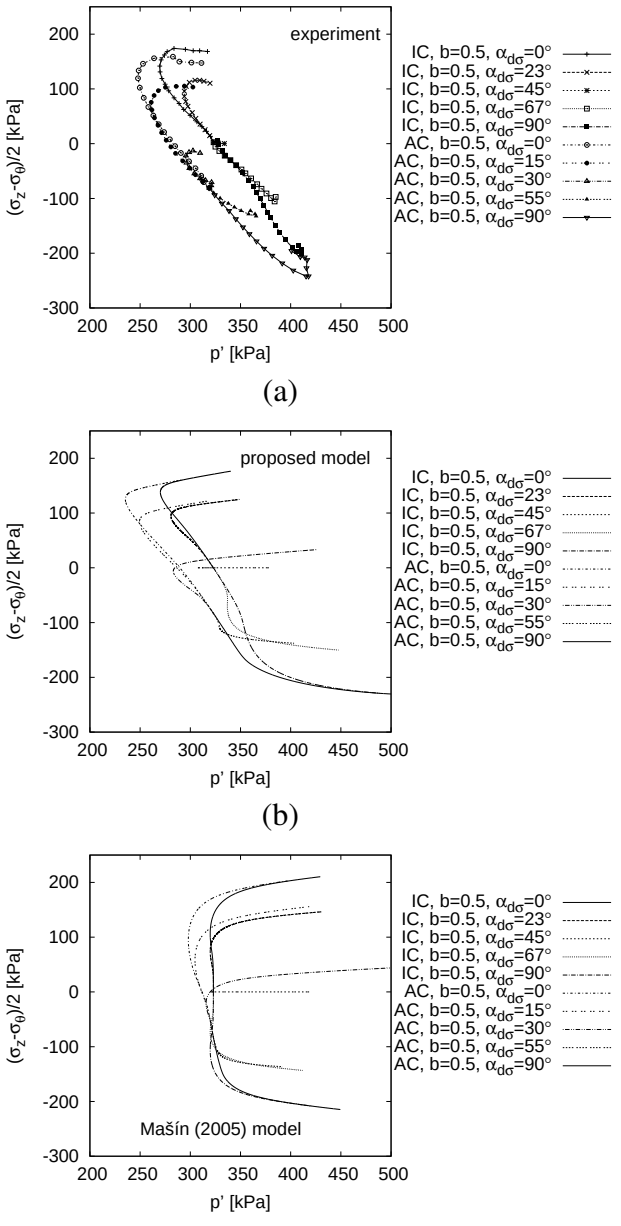

Figure 6: Stress paths in the p' vs. $(\sigma_z - \sigma_\theta)/2$ stress space: Experimental data by Nishimura et al. (2007), proposed model and Mašín (2005) model predictions.

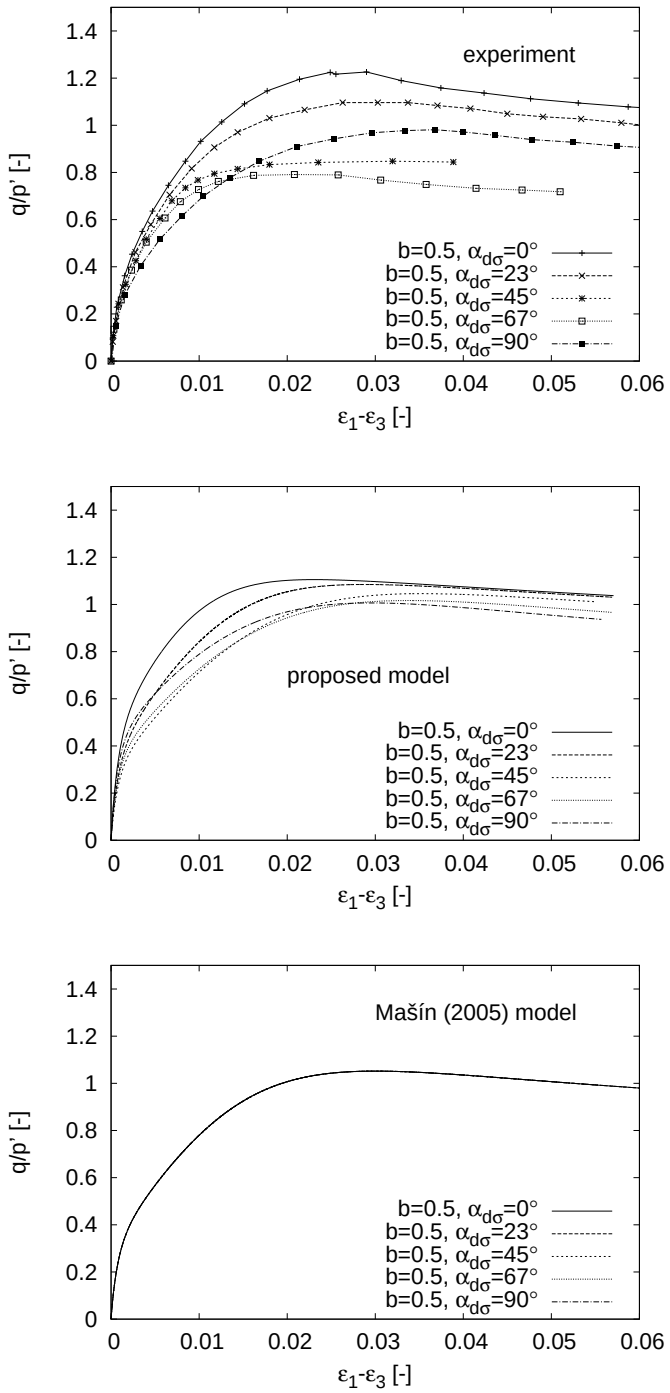

Figure 7: The ratio q/p' vs. the principal strain difference $\epsilon_1 - \epsilon_3$ for the IC series: Experimental data by Nishimura et al. (2007), proposed model and Mašín (2005) model predictions.

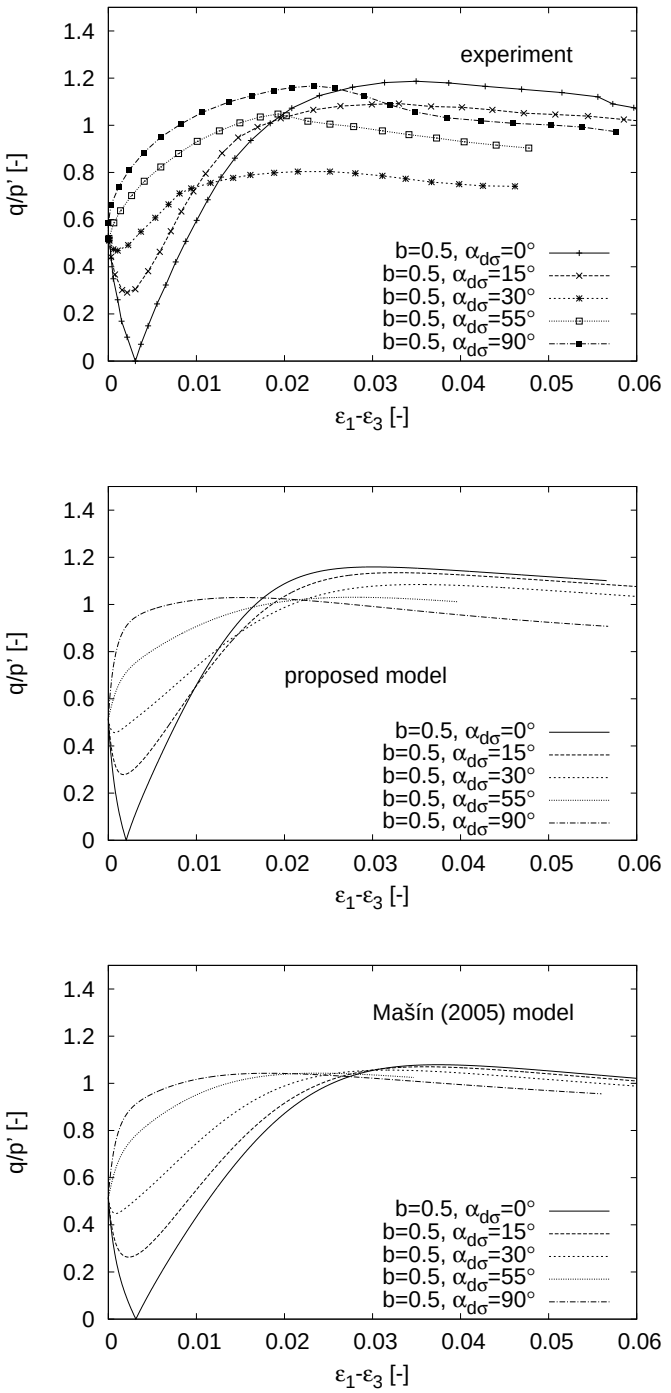

Figure 8: The ratio q/p' vs. the principal strain difference $\epsilon_1 - \epsilon_3$ for the AC series: Experimental data by Nishimura et al. (2007), proposed model and Mašín (2005) model predictions.

Finally, charts in Fig. 9 show strain evolution followed in the isotropically consolidated test with $b = 0.5$ and $\alpha_{d\sigma} = 23°$ (data from Nishimura (2005)). The models predict the strain evolution accurately. The anisotropy is revealed by slightly negative values of the radial strain ϵ_r, which are predicted by the proposed model only.

SUMMARY AND CONCLUSIONS

A new version of clay hypoplasticity model is presented for predicting stiffness anisotropy. The model is based on the reference model by Mašín (2012b), in which the stiffness tensor $\mathcal{L}$ is replaced by an anisotropic elasticity tensor. The model has been evaluated using comprehensive data set on London clay, which includes measurements of the influence of anisotropy in the hollow cylinder apparatus. It is demonstrated that the proposed model predicts not only the influence of anisotropy on the very small strain stiffness, but it also improves predictions of undrained stress paths.

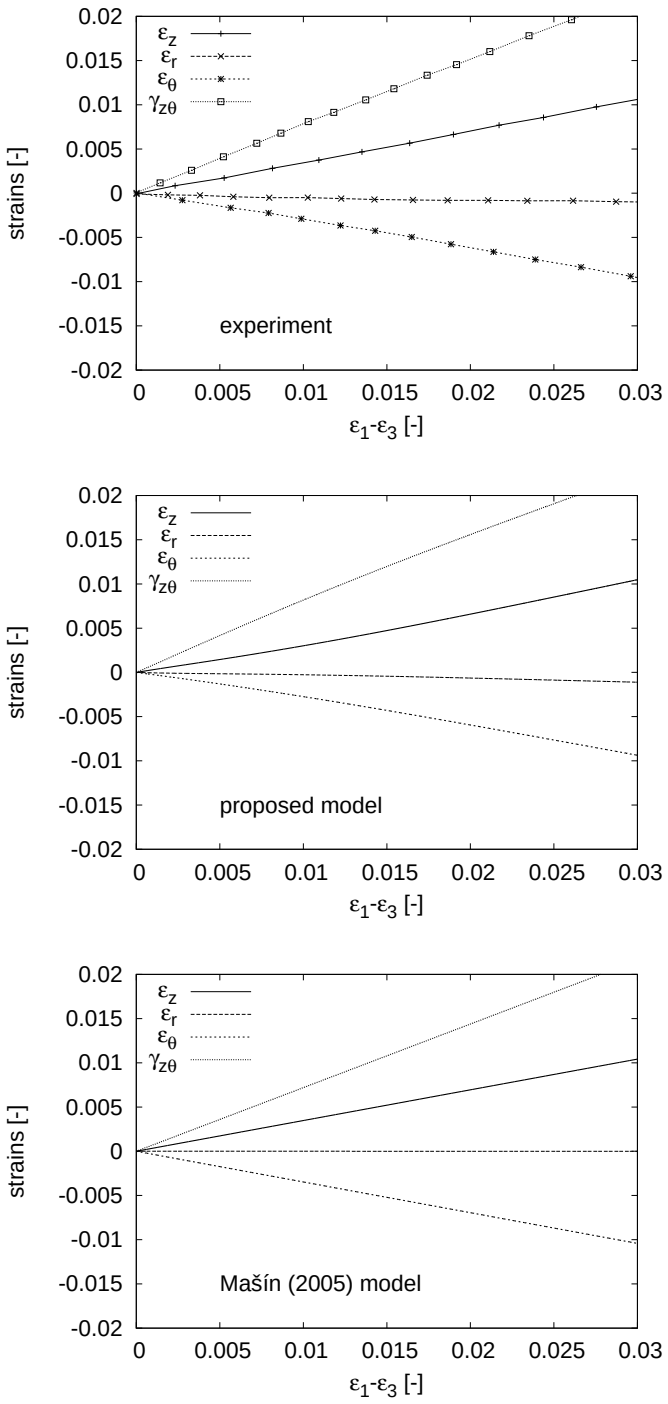

Figure 9: Strain paths measured in the isotropically consolidated test with $b = 0.5$ and $\alpha_{d\sigma} = 23°$. Experimental data by Nishimura (2005).

ACKNOWLEDGEMENT

Financial support by the research grant P105/12/1705 of the Czech Science Foundation is greatly appreciated.

REFERENCES

Addenbrooke, T., D. Potts, & A. Puzrin (1997). The influence of pre-failure soil stiffness on the numerical analysis of tunnel construction. *Géotechnique 47*(3), 693–712.

Franzius, J. N., D. M. Potts, & J. B. Burland (2005). The influence of soil anisotropy and K_0 on ground surface movements resulting from tunnel excavation. *Géotechnique 55*(3), 189–199.

Gasparre, A. (2005). *Advanced laboratory characterisation of London Clay*. Ph. D. thesis, University of London, Imperial College of Science, Technology and Medicine.

Gasparre, A., S. Nishimura, N. A. Minh, M. R. Coop, & R. J. Jardine (2007). The stiffness of natural London Clay. *Géotechnique 57*(1), 33–47.

Gudehus, G. (1996). A comprehensive constitutive equation for granular materials. *Soils and Foundations 36*(1), 1–12.

Gudehus, G., A. Amorosi, A. Gens, I. Herle, D. Kolymbas, D. Mašín, D. Muir Wood, R. Nova, A. Niemunis, M. Pastor, C. Tamagnini, & G. Viggiani (2008). The soilmodels.info project. *International Journal for Numerical and Analytical Methods in Geomechanics 32*(12), 1571–1572.

Gudehus, G. & D. Mašín (2009). Graphical representation of constitutive equations. *Géotechnique 59*(2), 147–151.

Gunn, M. J. (1993). The prediction of surface settlement profiles due to tunnelling. In G. T. Houlsby and A. N. Schofield (Eds.), *Predictive soil mechanics: Proceedings of the Worth Memorial Symposium, London*, pp. 304–316. Thomas Telford, London.

Lubarda, V. A. & M. C. Chen (2008). On the elastic moduli and compliences of transversely isotropic and orthotropic materials. *Journal of Mechanics of Materials and Structures 3*(1), 153–171.

Mašín, D. (2005). A hypoplastic constitutive model for clays. *International Journal for Numerical and Analytical Methods in Geomechanics 29*(4), 311–336.

Mašín, D. (2009). 3D modelling of a NATM tunnel in high K_0 clay using two different constitutive models. *Journal of Geotechnical and Geoenvironmental Engineering ASCE 135*(9), 1326–1335.

Mašín, D. (2012a). Asymptotic behaviour of granular materials. *Granular Matter 14*(6), 759–774.

Mašín, D. (2012b). Clay hypoplasticity with explicitly defined asymptotic states. *Acta Geotechnica 8*(5), 481–496.

Mašín, D. (2012c). Hypoplastic Cam-clay model. *Géotechnique 62*(6), 549–553.

Mašín, D. (2013). Clay hypoplasticity model including stiffness anisotropy. *Géotechnique (in print)*.

Mašín, D. & J. Rott (2013). Small strain stiffness anisotropy of natural sedimentary clays: review and a model. *Acta Geotechnica, DOI:10.1007/s11440-013-0271-2*.

Ng, C. W. W., E. H. Y. Leung, & C. K. Lau (2004). Inherent anisotropic stiffness of weathered geomaterial and its influence on ground deformations around deep excavations. *Canadian Geotechnical Journal 41*, 12–24.

Niemunis, A. & I. Herle (1997). Hypoplastic model for cohesionless soils with elastic strain range. *Mechanics of Cohesive-Frictional Materials 2*, 279–299.

Nishimura, S. (2005). *Laboratory study on anisotropy of natural London clay*. Ph. D. thesis, University of London, Imperial College of Science, Technology and Medicine.

Nishimura, S., N. A. Minh, & R. J. Jardine (2007). Shear strength anisotropy of natural London Clay. *Géotechnique 57*(1), 49–62.

Spencer, A. J. M. (1982). The formulation of constitutive equation for anisotropic solids. In J. P. Boehler (Ed.), *Mechanical behaviour of anisotropic solids*. Martinus Nijhoff Publishers, The Hague.

von Wolffersdorff, P. A. (1996). A hypoplastic relation for granular materials with a predefined limit state surface. *Mechanics of Cohesive-Frictional Materials 1*, 251–271.

Wroth, C. & G. Houlsby (1985). Soil mechanics - property characterisation, and analysis procedures. In *Proc. 11^{th} Conf. Soil. Mech., San Francisco*, Volume 1, pp. 1–55.